Absorption Less All-Optical Memory Cell Based on Active Micro Ring Optical Integrators

Nasibe Pasyar
Faculty of Electrical and Computer Engineering, University of Tabriz,Tabriz 5166615813, Iran.

Abstract. The three-level nano particles are doped in dual micro ring resonators of the proposed all-optical memory unit cell as the active gain segment in which the optical power loss is compensated due to the effect of lasing without inversion in doped quantum dots. The effect of parameters such as pumping rate and density of doped QDs are investigated. The optical integrator generates an optical step function to save input data. Also, the effect of electromagnetically induced transparency in three-level quantum dots is investigated as an on/off phase shifter for data reading at requested time. Both input data into the memory and output read pulse are return -to-zero Gaussian signals, but the output data has narrower pulse width. This is because of that the light in the integrator is mostly erased during the rising edge of the phase shift pulse. The proposed integrated memory cell can operate in high speed situations.

Keywords: Electromagnetically Induced Transparency, Lasing without Inversion, All-optical Memory cell, 3×3 Coupler, Ring Resonator.

***** Correspondence Author**,** E-mail: n_pasyar@tabrizu.ac.ir

1 Introduction

Optical memory, as an important element in future all optical computing and all optical network, is attracting wide attention. Most of current optical memory depends on the high nonlinear properties of materials such as silicon, whose optical properties can be changed upon triggered by light[1]. However, such kind of memory normally requires high operating power or complex structure. Due to the ever-increasing speed of fiber-optic-based telecommunications, the high-speed optical memories adapted to densely on-chip integration become critical for buffering of decisions and telecommunication data[2]. All-optical memory or buffer as a key element in optical packet switching (OPS) networks can resolve the packet contention problem. Tunable optical delay lines and optical memories as an important building blocks in advanced photonic integrated circuits (PICs) will offer the possibility to combine numerous optical functions including switching, modulation and amplification on a single substrate for optical information processing and all optical communication networks. Most of the optical buffering schemes such as slowing light, optical fiber loop and so on, produce a delay time of the data stream. The storage time in fiber loop optical memories, can be up to 1ms however, the setup is bulky because typically at least several meters long of fiber are required for the fiber loop[1,2].

Flip-flop memory is one kind of the most interesting memory types. However, it is still a great challenge to realize ultra-fast flip-flop operation with the switching time on picosecond time scale for GHz data memory[3]. Two SOA-based ON/OFF switches and two coupled semiconductor optical ampelifier- Mach Zender interferometer (SOA-MZI) gates forming an optical flip-flop has demonstrated an optical random access memory (RAM) cell[4].

Slow light devices have been extensively build using coupled resonator optical waveguides (CROW)[5,6]. Random access all-optical memory unit cells are also designed using ring resonators in which a data bit is stored in a resonator. It is shown that losses in the resonators, the extinction ratio and chirp of the variable coupling medium that injects and extracts data into and out of the resonators, and chirp on the input signal are the limiting factors in the resonator-based optical memories[7].The optomechanical effect between the silicon beam and the ring resonator is used to design the nano-optomechanical static RAM (SRAM) integrated with light modulation system on a single silicon chip in which bistability of silicon beam due to the non-linear optical gradient force generated from a ring resonator determens the memory states. The optical SRAM has write/read time around 120 ns, which is much faster as compared with traditional MEMS memory[8].

A memory unit cell has been presented[9,10] based on micro ring resonators in which electro absorption modulator (EAM) in Mach Zender interferometer (MZI) form operates as an optical switch. The proposed unit cell cannot operate as all-optical element and has large size to appear in integrated chip[1]. A dynamical slow light cell with dual-microring resonator configuration and far-field coupling has been demonstrated by controlling the group delay through thermo-optically detuning the resonant frequencies of the two rings in which usable group delays up to 24 ps are measured, with losses <1dB[11].

In this paper, active microring resonators doped with three level quantum dots (QDs) and directional couplers as optical integrators are used to design an all-optical memory unit cell in which Electromagnetically Induced Transparency (EIT) and Lasing Without Inversion (LWI) techniques are applyed to make a delay line to achieve required phase shift and amplify optical pulse, respectively. A single optical integrator generates an optical step function for the Gaussian input pulse[10]. The proposed dual optical integrators can realize a scheme of controllable optical memory unit, with a phase shift element introduced for the data reading control. The compact size for densely integration and large-scale data storage and being very convenient to be cascaded are the main advantage of such optical memory unit. Secondly the read operation is controllable, the data bit can be read out at any time needed, and the read-out response time of the read operation is very fast. The high speed operations in picoseconds scale is demonstrated. The main advantage of the optical integrator-based memory compared to the flip-flop memory, is that the rising edge is the cumulative time integral of the input pulse, so it is as fast as the bit rate, and this performance is very important for the high speed data storage. Here, LWI in three-level nanoparticles doped to the ring resonator as the active gain mediume for optical power loss in data storage and EIT technique for the required phase shift for data read has been processed and the effect of parameters such as pumping rate and doped QDs density has been investigated. Thus, this designed all-optical memory unit cell can work in low power high-speed situations.

2 Integrator Structure

an optical integrator with power coupling coefficient α' of the directional coupler is shown in Fig. 1. The field in the resonator is assumed to propagate in the counter clockwise direction. When light propagates a round-trip or a sampling period T, the field is enhanced due to the positive feedback until all the input light pulse is injected. After that the light intensity is still kept on, because of the loss compensation supplied by the active gain medium.

By doping 3-level nanocrystals (quantum dots) into gain and phase shifter segments in ring resonator and using LWI and EIT techniques we get the required gain and phase shift to read out the stored data. Fig. 1 illustrates Λ type 3-level nanoparticles doped into ring resonator as the gain segment. The control field is applied in resonant with $|2\rangle$ - $|3\rangle$ transition and the probe field is applied to $|1\rangle$ - $|3\rangle$ transition respectively.

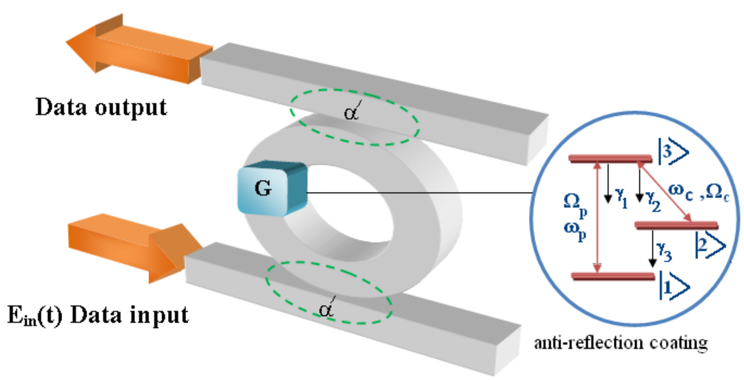

Fig. 1 The scheme of an optical integrator with three level Λ-type QD as gain segment.

2.1 Electromagnetically Induced Transparency and Lasing without Inversion process

In 3-level QD configuration considered in Fig. 1 the levels $|1\rangle$ and $|3\rangle$ are coupled by probe field of amplitude E_p and frequency ω_p, whose dispersion and absorption we are interested. Level $|2\rangle$ is coupled to level $|3\rangle$ by a strong control field of frequency ω_c.

The Hamiltonian[12] of three-level Λ-type atomic system can be written as:

$$H = \hbar(\omega_{13}|3\rangle\langle 3|) + (\hbar\omega_{12})|2\rangle\langle 2| - \frac{\hbar}{2}(\Omega_P e^{-i\varphi_p} e^{-i\nu_p t}|3\rangle\langle 1| + \Omega_c e^{-i\varphi_c} e^{-i\nu_c t}|3\rangle\langle 2|) + H.c. \tag{1}$$

where, $\nu_p, \nu_c, \hbar, \hbar\omega_{13}, \hbar\omega_{12}, \Omega_p e^{-i\varphi_p}, \Omega_c e^{-i\varphi_c}, H.c.$ are the probe field frequency, control field frequency, the reduced plank constant, energy of atomic level $|3\rangle$, energy of atomic level $|2\rangle$, complex Rabi frequency of the probe field coupled to atomic transition $|1\rangle$ - $|3\rangle$, complex Rabi frequency of the control field coupled to atomic transition $|3\rangle$ - $|2\rangle$, Hermitian conjugate, respectively.

With the substitution of $\Omega_P e^{-i\varphi_p} = \frac{\wp_{31} E_p}{\hbar}$, where, Ã $_{13}$is dipole moment element and based on the Hamiltonian, equations of motion for the density matrix elements can be expressed as:

$$\frac{\partial \rho_{31}}{\partial t} = -(\gamma_1 + i\Delta)\rho_{31} + \frac{i\wp_{31}\mathrm{E}_p}{\hbar} + \frac{i}{2}\Omega_c e^{-i\varphi_c}\rho_{21}, \tag{2}$$

$$\frac{\partial r_{21}}{\partial t} = -(g_3 + i\mathrm{D}) r_{21} + \frac{i}{2}\mathrm{W}_c e^{ij_c} r_{31}, \tag{3}$$

Solving the coupled set of equations , the time dependent density matrix element is written as:

$$\rho_{31}(t) = \frac{i\wp_{31}\mathrm{E}_p(\gamma_3 + i\Delta)}{2\hbar\left[(\gamma_1 + i\Delta)(\gamma_3 + i\Delta) + \Omega_c^2/4\right]}, \tag{4}$$

The linear susceptibility of the system is:

$$c = \frac{P}{e_0 E} = 2\left(\frac{\wp_{13} r_{31}}{e_0 E} + \frac{\wp_{23} r_{32}}{e_0 E}\right) e^{int}, \tag{5}$$

Using the relation of polarization in Eq. 5, and by using the density matrix approach and rate equations, one can find the electromagnetically susceptibility of the medium as a function of the weak probe field. The imaginary part of susceptibility, Im(c) determines the absorptive properties of medium and the real part, $\mathrm{Re}(c)$ is related to the refractive index. So, for the case of EIT by using the Eqs. 2, 3 and Eq.5 the following expression for real and imaginary parts of the complex optical susceptibility is obtained[12-15].

$$\chi' = \frac{N_a \wp_{31}^2 \Delta}{\varepsilon_0 \hbar Z}[\gamma_3(\gamma_1+\gamma_3)+(\Delta^2-\gamma_1\gamma_3-\Omega_c^2/4)], \tag{6}$$

$$\chi'' = \frac{N_a \wp_{31}^2}{\varepsilon_0 \hbar Z}[(\Delta^2(\gamma_1+\gamma_3)-\gamma_3(\Delta^2-\gamma_1\gamma_3-\Omega_c^2/4)], \tag{7}$$

$$\begin{cases} \Omega_c = \dfrac{\wp_{32} E_c}{\hbar}, \\ Z = (\Delta^2-\gamma_1\gamma_2-\Omega_c^2/4)^2+\Delta^2(\gamma_1+\gamma_2)^2. \end{cases} \tag{8}$$

where, $\nu, \Delta=\omega_{31}-\nu, \Omega_c, \varepsilon_0, \hbar, \wp_{32}, \kappa, n, c, N_a, \gamma_1, \gamma_2, \gamma_3$ are the probe field frequency, resonance detuning of $|1\rangle$ - $|3\rangle$,Rabi frequency, vacuum dielectric constant, reduced plank constant, dipole moment element of $|3\rangle$ - $|2\rangle$, propagation wave vector, refractive index of the wavegiude, optical wave velocity in vacuum, atomic density of doped nanocrystals and atomic decay rates, respectively.

For the analysis of lasing without inversion (LWI), a single mode field of frequency υ and complex amplitude E(t) interacts with the three-level atomic system, so the interaction Hamiltonian in with some substitutions is written as the following:

$$H = \hbar(\omega_{13}|3\rangle\langle 3|)+(\hbar\omega_{12})|2\rangle\langle 2|-\frac{\hbar}{2}(\frac{\wp_{31}\mathrm{E}(t)}{\hbar}e^{-i\nu t}|3\rangle\langle 1|+\frac{\wp_{32}\mathrm{E}(t)}{\hbar}e^{-i\nu t}|3\rangle\langle 2|)+H.c. \tag{9}$$

In this case the equations of motion for the elements of the population matrix[12,15] are given by:

$$\frac{\partial\rho_{31}}{\partial t} = -(i\omega_{31}+\gamma_{31})\rho_{31}-\frac{i\wp_{31}\mathrm{E}(t)}{2\hbar}e^{-i\nu t}(\rho_{33}-\rho_{11})+\frac{i\wp_{32}\mathrm{E}(t)}{2\hbar}e^{-i\nu t}\rho_{21}, \tag{10}$$

$$\frac{\partial\rho_{32}}{\partial t} = -(i\omega_{32}+\gamma_{32})\rho_{32}-\frac{i\wp_{32}\mathrm{E}(t)}{2\hbar}e^{-i\nu t}(\rho_{33}-\rho_{22})+\frac{i\wp_{31}\mathrm{E}(t)}{2\hbar}e^{-i\nu t}\rho_{12}, \tag{11}$$

$$\frac{\partial \rho_{33}}{\partial t} = r_a \rho_{33}^{(0)} - \gamma_3 \rho_{33}, \tag{12}$$

$$\frac{\partial \rho_{11}}{\partial t} = r_a \rho_{11}^{(0)} - \gamma_1 \rho_{11}, \tag{13}$$

$$\frac{\partial \rho_{22}}{\partial t} = r_a \rho_{22}^{(0)} - \gamma_2 \rho_{22}, \tag{14}$$

$$\frac{\partial \rho_{12}}{\partial t} = r_a \rho_{12}^{(0)} - (i\omega_{12} + \gamma_{12})\rho_{12}, \tag{15}$$

Where, r_a is the pumping rate. The euation of motion for the field amplitude is given by:

$$\frac{\partial E(t)}{\partial t} = -\frac{\nu}{\varepsilon_0} \mathrm{Im}\{e^{i\nu t}[\wp_{23}\rho_{32}(t) + \wp_{13}\rho_{31}(t)]\}, \tag{16}$$

We assume E(t) to be slowly varying function of time.

For certain choices of parameters, the absorption terms proportional to ρ_{11} and ρ_{22} will cancel the coherence terms proportional to ρ_{12} and ρ_{21} leading to lasing without inversion. This happens in the case that:

$$\begin{gathered} \gamma_2 = \gamma_1 = \gamma_3 = \gamma, \quad \wp_{32} = \wp_{31} = \wp, \\ \gamma > \omega_{12}, \quad \rho_{12}^{(0)} = \left|\rho_{21}^{(0)}\right| e^{i\pi}, \end{gathered} \tag{17}$$

and

$$\begin{gathered} \gamma_3 < \gamma_1, \quad \gamma_2 = \gamma_1 = \gamma, \quad \wp_{32} = \wp_{31} = \wp, \\ \gamma = \omega_{31}, \quad \rho_{12}^{(0)} = \left|\rho_{21}^{(0)}\right| e^{i3\pi/2}, \end{gathered} \tag{18}$$

Based on basic relations of optical susceptibility in Eqs. 6, 7 with gain and refractive index, the following relations are written[13].

$$g = -\frac{k}{2}\chi'', \delta n = n\frac{\chi'}{2}, \tag{19}$$

$$n_{eff} = n + \delta n, \tag{20}$$

2.2 Memory Statics

Two micro rings doped by 3-level nanoparticles as the LWI gain mediums in Fig. 2 are optical integrators with the same size and are coupled via a 3 ×3 coupler. However, the upper integrator has an EIT phase shifter, implemented by an intensive optical control field which plays a critical role for the data writing and reading operations. The data pulse is injected into the input port and splitted into two beams by a lossless and polarization independent 50:50 splitter. The phase of the lower beam is changed by π/2 after the splitter, and an additional π/2 phase shift is introduced into the lower beam. So, the phase difference between two beams is π before being injected into the optical integrators. The light fields injected into the upper and lower integrators are $E_{in}(t)/\sqrt{2}$ and $-E_{in}(t)/\sqrt{2}$, respectively. The light fields stored in the upper and lower integrators are represented by $E_4(t)$ and $E_6(t)$, respectively. The output field from the memory unit is denoted by $E_5(t)$. The amplitude and phase propagation equations[10] are described as:

$$\begin{aligned} \frac{\partial E_i}{\partial z} &= (g-\alpha)E_i, \qquad i=(u,d) \\ \frac{\partial \varphi}{\partial z} &= k_{eff}, \end{aligned} \tag{21}$$

$$k_{eff} = \frac{2\pi\nu n_{eff}}{c}, \tag{22}$$

where, k_{eff}, g, α and n_{eff} are the effective wave number of the field, gain coefficient, optical loss of the microring resonator and effective refractive index, respectively.

Assuming that the location of the phase shifter is z_p, the output light phase of the phase shifter and the light field in the 2 × 2 coupler satisfy the following relations[10]:

$$\varphi_{phaseshifter} = \varphi(z=z_p) + \Delta\varphi(t), \tag{23}$$

$$E_i' = \sqrt{1-\alpha'}E_i - j\sqrt{\alpha'}E_{in}^{\,i} \tag{24}$$

where, E^{i}_{in} is the optical data stream injected into the optical integrator, and E_{in} is the input field at the input port of the memory unit.

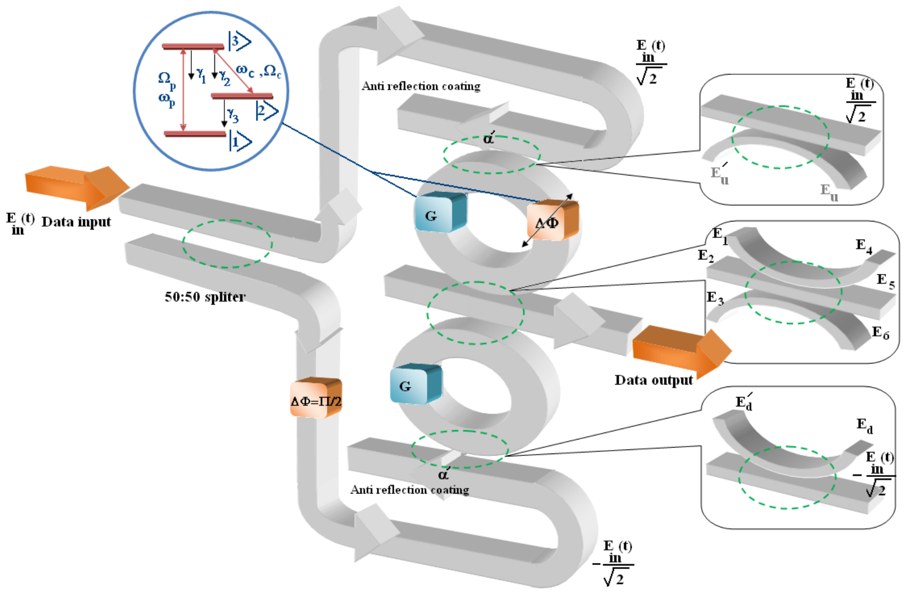

Fig. 2 The proposed all-optical memory cell.

The following transfer functions are considered for 3×3 couplers[14,15]:

$$\begin{bmatrix} E_4 \\ E_5 \\ E_6 \end{bmatrix} = T \begin{bmatrix} E_1 \\ E_2 \\ E_3 \end{bmatrix} = \begin{bmatrix} \left(\cos\left(\sqrt{2}h_0\right)+1\right)\big/2 & i\sqrt{2}\sin\left(\sqrt{2}h_0\right)\big/2 & \left(\cos\left(\sqrt{2}h_0\right)-1\right)\big/2 \\ i\sqrt{2}\sin\left(\sqrt{2}h_0\right)\big/2 & \cos\left(\sqrt{2}h_0\right) & i\sqrt{2}\sin\left(\sqrt{2}h_0\right)\big/2 \\ \left(\cos\left(\sqrt{2}h_0\right)-1\right)\big/2 & i\sqrt{2}\sin\left(\sqrt{2}h_0\right)\big/2 & \left(\cos\left(\sqrt{2}h_0\right)+1\right)\big/2 \end{bmatrix} \begin{bmatrix} E_1 \\ E_2 \\ E_3 \end{bmatrix}, \quad (25)$$

where, h_0 characterizes the coupling strength between two adjacent waveguides in 3×3 couplers. The coupler is designed as $h_0 = \sqrt{2}p\big/4$, thus the transfer function of 3×3 coupler is reduced as[10,15]:

$$H_{\mathrm{int}}(\omega)=\frac{E_4(\omega)}{E_{in}(\omega)}=\frac{\sqrt{2}}{2}\frac{j[G\alpha^{'}\exp(-\gamma L)]^{1/2}\exp(-j\omega T/2)}{1-\frac{1}{2}(\exp(j\Delta\varphi(t))+1)[G(1-\alpha^{'})\exp(-2\gamma L)]^{1/2}\exp(-j\omega T)}, \tag{26}$$

$$H_{out}(\omega)=\frac{E_5(\omega)}{E_{in}(\omega)}=-\frac{1}{2}(\exp(j\Delta\varphi(t))-1)\times\frac{[G^2\alpha^{'}(1-\alpha^{'})\exp(-2\gamma L)]^{1/2}\exp(-j3\omega T/2)}{1-\frac{1}{2}(\exp(j\Delta\varphi(t))+1)[G(1-\alpha^{'})\exp(-2\gamma L)]^{1/2}\exp(-j\omega T)}, \tag{27}$$

where, $G,\alpha',\gamma,L,\omega,T$ and $\Delta\varphi$ are optical gain, power coupling coefficient, waveguide loss, length of ring resonator, angular frequency of the optical pulse, loop delay in ring resonator and magnitude of phase shift in phase shifter segment, respectively. Initially the phase shifter is adjusted to $\Delta\varphi(t)=0$. Thus, there is no light at the output port 5 and the data is stored in the micro ring integrator and $\mathrm{H}_{out}(\omega)=0$. If the phase shifter is turned to $\Delta\varphi(t)=\theta$ under gain matching condition, after a round trip from port 4 (6) to 1 (3), fields are changed and given by:

$$\begin{bmatrix} E_4 \\ E_5 \\ E_6 \end{bmatrix}=T\begin{bmatrix} E_1 \\ E_2 \\ E_3 \end{bmatrix}=\exp(-j\omega T)\begin{bmatrix} \cos(\theta/2)E_{\mathrm{int}}\exp(j\theta/2) \\ -\sqrt{2}\sin(\theta/2)E_{\mathrm{int}}\exp(j\theta/2) \\ -\cos(\theta/2)E_{\mathrm{int}}\exp(j\theta/2) \end{bmatrix} \tag{28}$$

The remaining light intensity in the integrator and output port after N round trips is written as:

$$I_{\mathrm{int}}(t_0+NT)=\left|\prod_{j=1}^{N}\cos(\Delta\varphi(t_0+jT)/2)E_{\mathrm{int}}\right|^2 \tag{29}$$

$$I_{out}(t_0+NT)=\left|\sqrt{2}\sin(\Delta\varphi(t_0+(N-1)T)/2)\prod_{j=1}^{N}\cos(\Delta\varphi(t_0+(j-1)T)/2)E_{\mathrm{int}}\right|^2 \tag{30}$$

3 Simulation Results

This section consists of the simulation results based on numerical investigation for the proposed all-optical memory. After the illustration of optical susceptibility of three level QDs, the simulation results of the gain medium implemented by LWI effect and the phase shift realized by EIT are considered. Finally, the operation of optical memory is illustrated.

The real and imaginary parts of the optical susceptibility of doped QDs (Gain segments) in the case of LWI, versus wavelength are illustrated in Fig. 3 for different values of pumping rates (10, 12.5, 15.6, 19.5 and 24.4GHz) and parameter values of, $N_a = 10^{16}\mathrm{cm}^{-3}$, $g_1 = g_2 = 1THz, g_3 = 1GHz$.

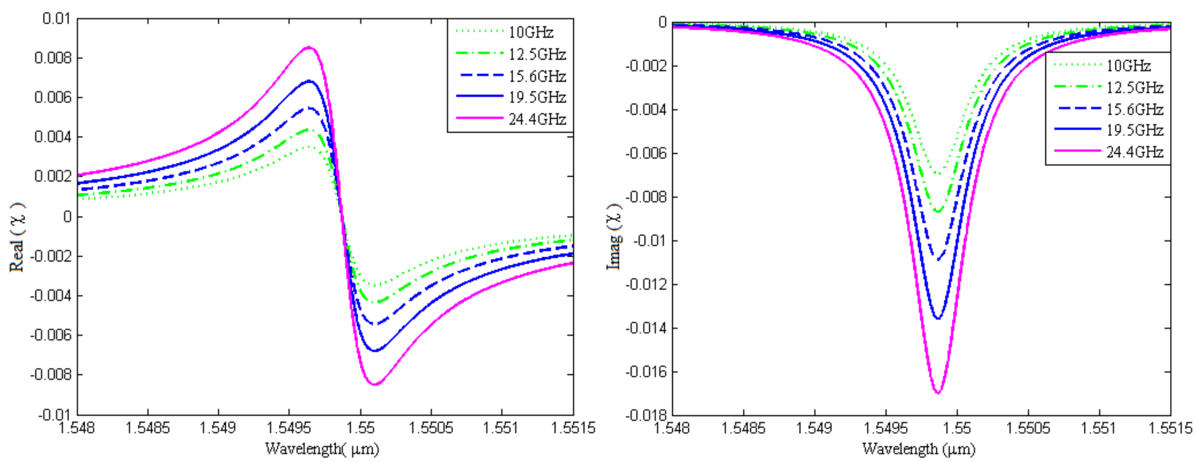

(a) **(b)**

Fig. 3 (a) Real and (b) Imaginary parts of the susceptibility for different pumping rates.

The real part of susceptibility, Re(c), in Fig.3a is related to the refractive index and the imaginary part of susceptibility, Im(c) in Fig.3b determines the absorptive properties of medium and. So, The it is proportinal to absorbsion and the negetive Im(c) means the existance of the gain. According to Fig.3 by increasing the pumping rates the susceptibility increases.

The gain profile of LWI of the gain segments in the integrators for different values of pumping rates (10, 12.5, 15.6, 19.5 and 24.4GHz) and parameter values of, $N_a = 10^{16}$ cm^{-3}, $g_1 = g_2 = 1THz, g_3 = 1GHz$ is illustrated in Fig. 4a. It is observed that by increasing the pumping rate the LWI gain increases. Also, it is clear that these gain segments in spite of amplifying the optical pulse as much as required, can operate as a sharp filter.

The gain profile verses the effective wave number for doped QDs densities of $1.0\times10^{16}, 7\times10^{15}, 9\times10^{15}$cm^{-3} has been illustrated in Fig. 4b. It is observed that the gain of active medium increases as the number of doped QDs increases.

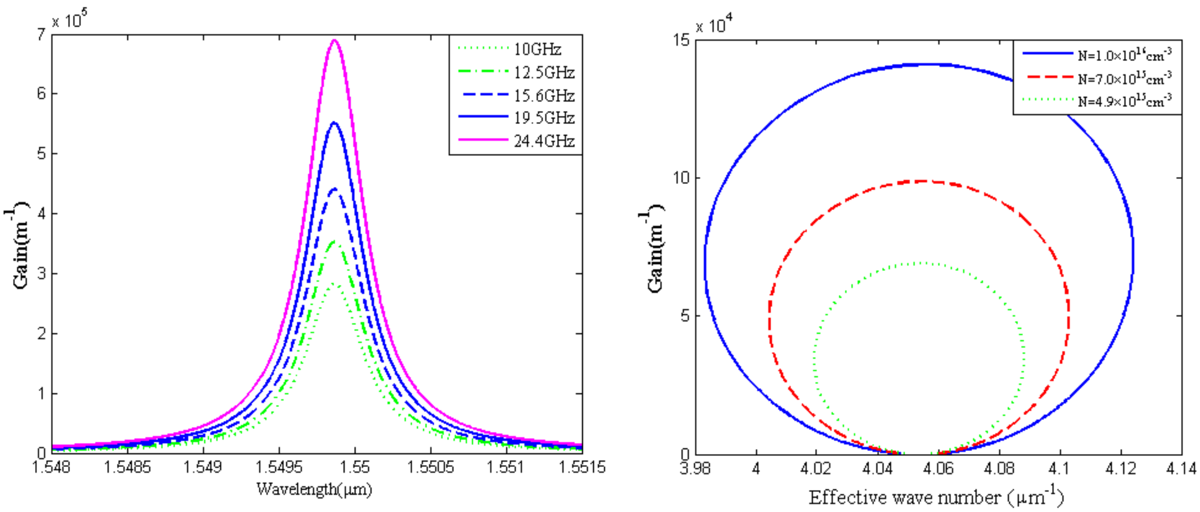

(a) **(b)**

Fig. 4 (a) The gain profile of the gain segments in integrators for different values of the pumping rate. (b) The gain profile of the gain segments verse the effective wave number for different numbers of doped QDs.

Figure. 5 illustrates the electromagnetically induced transparency (EIT) applied as optical phase shifter with the following parameter values of the phase shifter. $N_a = 1.5´\ 10^{18}$ 1/cm^3, $Ã_{ba} = Ã_{ca} = 5´\ 10^{-27}$ coulomb.meter, $g_1 = 60GHz, g_3 = 0.1MHz, W_c = 0.3THz$.

By applying the control field the phase shifting is realized due to EIT phenomena. Fig. 5 shows the phase and gain profiles of the phase shifter segment for two cases of with and without control field.

In absence of the control field, the signal field, which interacts with the resonant two-level system, undergoes partial or complete absorption. In presence of the control field, the absorption of the signal is greatly reduced. So, for resonance frequencies near the two photon Raman resonances the electromagnetically induced transparency (EIT) is obtained. Also, the sharp drop filtering properties is observed in doped QDs phase shifter.

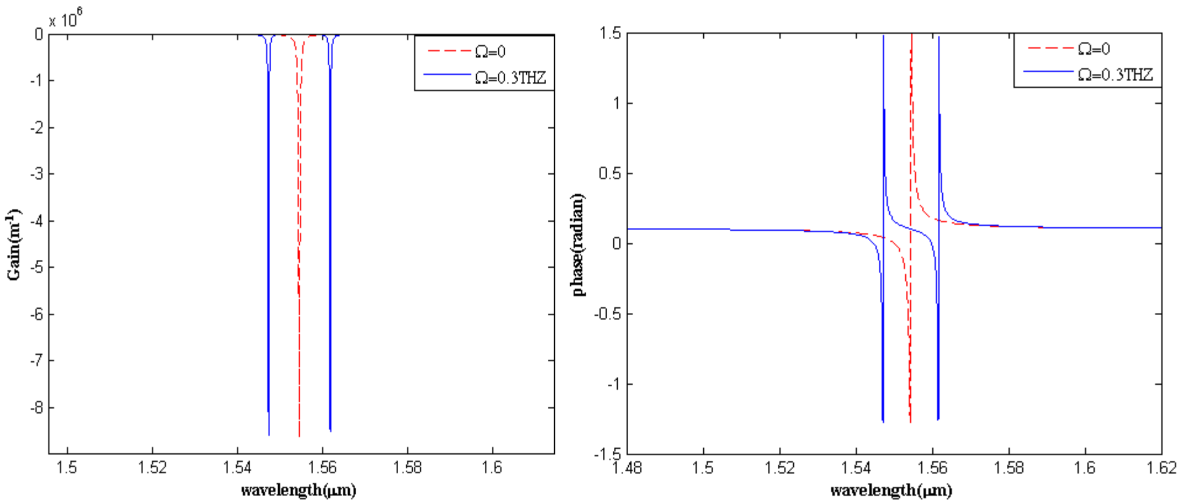

Fig. 5 (a) Phase and (b) Gain profiles of the phase shifter segment**.**

Figure. 6 illustrates the electromagnetically induced transparency (EIT) applied as optical phase shifter with the following parameter values of the phase shifter. $N_a = 1.5\times 10^{18}$ 1/cm^3, $\tilde{A}_{ba} = \tilde{A}_{ca} = 5\times 10^{-27}$ coulomb.meter, $g_1 = 60GHz$, $g_3 = 0.1MHz$, $W_c = 1.2THz$. Transparency profile of the phase shifter segment for two cases of with and without control field is presented in Fig. 6a.

The phase profile of phase shifter segment is illustrated in Fig. 6b. It is obvious that the required phase shift, $\pi/2$, (which is necessary for reading the stored data) in EIT window about

1550nm wavelength can be realized by applying the control field. Whenever the control field is applied, a $\pi/2$ phase shift can be achieved at 1550nm with negligible amount of absorption.

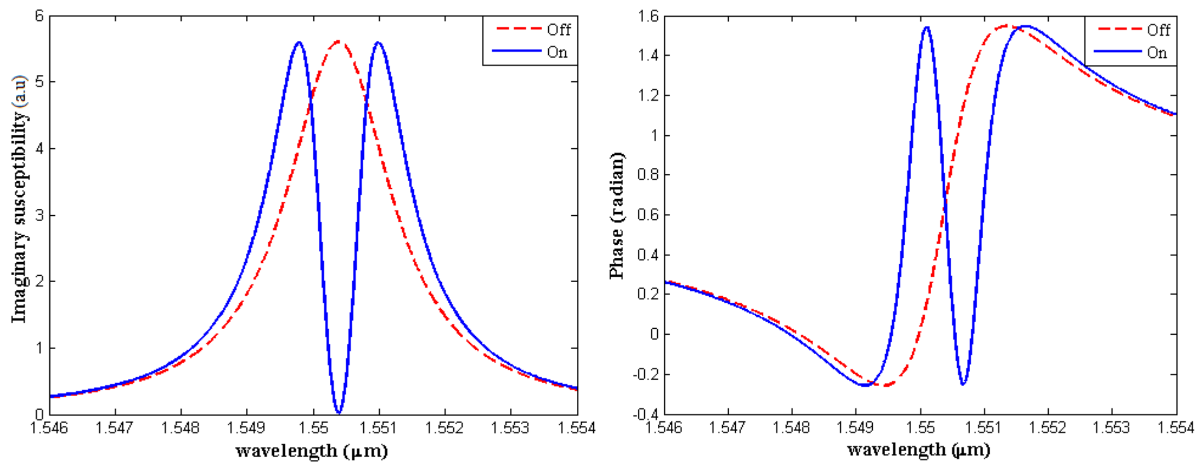

(a) **(b)**

Fig. 6 (a) Transparency (b) phase profiles of the phase shifter with and without control field.

The data storing and read out process of the proposed all-optical memory unit cell with the parameters of power coupling coefficient (α'=0.5), refractive index of the fiber n=2.8, λ=1550nm, length of rings L=1µm is illustrated in Fig. 7. The input Gaussian pulse to the all-optical memory cell is presented in Fig. 7a. The input pulse is saved with a step function shape in integrators as the storage process in Fig. 7b. Finally, it is observed in Fig. 7c that whenever the required phase shift is occurred by applying the control field of the phase shifter segment, the stored data we can be read out.

By considering the Figs. 7b- 7c one can see that by applying the required phase shift, the input pulse is occurred in the output port and the integrators are deleted from data. Since, the light in the integrator is mostly erased during the rising edge of the phase shift pulse so, the FWHM of the data read out is about 10.5ps, a little narrower than half of the FWHM of the phase shift pulse with a value of 21.5ps.

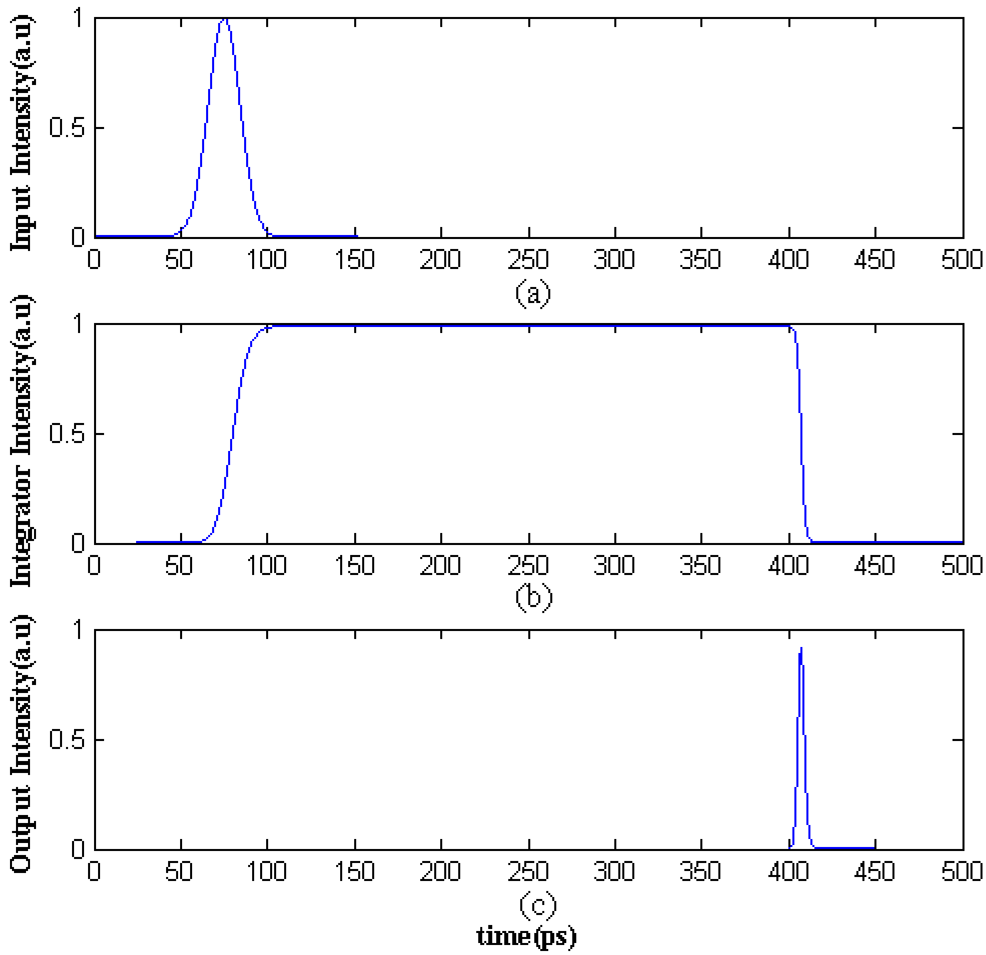

Fig. 7 Data storing and read out process of optical memory unit cell, a) input pulse, b) Saved data, c) output pulse. Power coupling coefficient (α'=0.5), refractive index of the fiber n=2.8, λ=1550nm, length of rings L=1μm.

4 Conclusion

3-level QDs are doped in ring resonators used in the memory unit cell to realize EIT and LWI phenomena to achieve the required phase shift and gain in all-optical memory unit. The effect of parameters such as pumping rate and density of doped QDs on susceptibility and LWI gain are investigated. Also, the data storing and read out process of optical memory unit cell is illustrated. The compact size for integrated purposes without necessity to add optical filter for high speed operation and higher speed of designed memory compared with the previously reported approaches are the significunt specifications of the proposed memory cell.

References

1. S.N.Fu, P.Shum, G.Ning, C.Q.Wu, and Y.J.Li, "Theoretical investigation of dual-Wavelength packet signal storage with SOA-based dual loop optical buffer," *Opt. Communications*, **279**(2), 255–261 (2007).
2. Q. F. Xu, P. Dong, and M. Lipson, "Breaking the delay-bandwidth limit in a photonic structure," *Nat. Phys.* **3**(6), 406–410 (2007).
3. Reis C., Maziotis A., Kouloumentas C., Stamatiadis C., Calabretta N., Andre P. S., Dionisio R.P., Neto B., Dorren H. J. S., Avromopoulos H., Teixeira A. "All-optical clocked D flip-flop memory using a hybrid integrated S-R latch" *Microwave Op. Tech. Letters*, **53**(6), 1201-1204 (2011).
4. D. Fitsios, K. Vyrsokinos, A. Miliou, N. Pleros, "Memory Speed Analysis of Optical RAM and Optical Flip-Flop Circuits Based on Coupled SOA-MZI Gates," *Selected Topics in Quantum Electronics, IEEE* **18**(2) , 1006 – 1015 (2012).
5. P.Narmadhadevi, D.Shanmuga Sundar, L.Malathi, "Performance Analysis of Different Micro Ring Resonators based on Optical Delay Lines," *International Journal of Computer Applications*, **67**(13), 0975 – 8887 (2013).
6. A. W. Elshaari, A. Aboketaf, and S. F. Preble, "Controlled storage of light in silicon cavities," *Optics Express*, **18**(3), 3014-3022 (2010).
7. R. S. Tucker, and J. L. Riding, "Optical ring-resonator random-access memories," *IEEE J. lightwave Technology*, **26**(3), 320–328 (2008).
8. B. Dong, H. Cai, Y.D. Gu, Z.C. Yang, Y.F. Jin, Y.L. Hao, D.L. Kwong, A.Q. Liu," Nano-optomechanical static random access memory (SRAM)", *2015 28th IEEE International Conference on Micro Electro Mechanical Systems (MEMS)*, pp. 49 – 52, Estoril,(2015). [doi: 10.1109/MEMSYS.2015.7050883].

9. Yunhong Ding, Xiaobei Zhang, Xinliang Zhang and Dexiu Huang, “Proposal for loadable and erasable optical memory unit based on dual active microring optical integrators”, *Optics Communications*, **281**(21), 5315-5321 (2008).
10. Yunhong Ding, Xiaobei Zhang, Xinliang Zhang, and Dexiu Huang, “Active microring optical integrator associated with electroabsorption modulators for high speed low light power loadable and erasable optical memory unit ”, *optics express*, **17**(15), 12835-12848 (2009).
11. Marcus S. Dahlem, Charles W. Holzwarth, Henry I. Smith, Erich P. Ippen, and Miloš A. Popović, “Dynamical Slow Light Cell based on Controlled Far-Field Interference of Microring Resonators,” OSA/IPR/PS, IMC4, (2010).
12. See, e.g., M.O. Scully, M.S. Zubairy, “*Quantum Optics*,” Cambridge University. Press, Cambridge, (1997).
13. K. Kowalski, V. cao Long, K. DinhXuan, M. Glodz, B. Nguyen, J.Szonert, **"**Electromagnetically Induced Transparency**"** *Computational Methods in science and Technology*, **SI**(2), 131-145 (2010).
14. X.B. Zhang, D.X. Huang, X.L. Zhang,”Transmission characteristics of dual microring resonators coupled via 3×3 couplers”, *Opt. Express*, **15**(21), 13557-13573 (2007).
15. N Pasyar, R.Yadipour, and H. Baghban ," Design of All-Optical Memory Cell Using EIT and Lasing Without Inversion Phenomena in Optical Micro Ring Resonators" *optics communications*, **395** ,241-248 (2017).